Formation of Polymorphic Cluster Phases for a Class of Models of Purely Repulsive Soft Spheres

Bianca M. Mladek,[1] Dieter Gottwald,[1] Gerhard Kahl,[1] Martin Neumann,[2] and Christos N. Likos[3]
[1]*Center for Computational Materials Science and Institut für Theoretische Physik, Technische Universität Wien, Wiedner Hauptstraße 8-10, A-1040 Wien, Austria*
[2]*Institut für Experimentalphysik, Universität Wien, Strudlhofgasse 4, A-1090 Wien, Austria*
[3]*Institut für Theoretische Physik II, Heinrich-Heine-Universität Düsseldorf, Universitätsstraße 1, D-40225 Düsseldorf, Germany*
(Received 7 November 2005; published 30 January 2006)

We present results from density functional theory and computer simulations that unambiguously predict the occurrence of first-order freezing transitions for a large class of ultrasoft model systems into cluster crystals. The clusters consist of fully overlapping particles and arise without the existence of attractive forces. The number of particles participating in a cluster scales linearly with density, therefore the crystals feature density-independent lattice constants. Clustering is accompanied by polymorphic bcc-fcc transitions, with fcc being the stable phase at high densities.

DOI: 10.1103/PhysRevLett.96.045701 PACS numbers: 64.70.Dv, 61.20.Ja, 82.30.Nr, 82.70.Dd

The distinguishing feature of soft matter systems is the vast separation of length and time scales characterizing the extent and motion of their constituent entities. The solvent is microscopic whereas the solute particles are mesoscopic [1]. The ability to control the architecture and chemical nature of these macromolecules, combined with the flexibility in influencing the solvent properties and the composition of the system, gives rise to an unprecedented freedom in tuning the effective interactions between the particles and opens up the possibility of steering the macroscopic properties of the system [1,2]. The richness of spontaneously forming complexes in soft matter encompasses length scales that exceed the dimensions of the individual macromolecules. Indeed, the latter can self-organize in a variety of ways, giving rise to so-called *hypermolecular* structures [3] that encompass a large number of mesoscopically sized entities. Characteristic examples are the complex phases encountered in ternary mixtures of oil, water, and amphiphilic surfactants or in block copolymer blends, as well as the emergence of *cluster formation* between colloidal particles, which has attracted a great deal of attention recently [4–12]. The underlying physical mechanism that drives the emergence of hypermolecular structures is widely believed to rest on the existence of competing interactions among the mesoscopic solute constituents. For example, the dominant mechanism that guarantees the stability of finite clusters in colloidal [5,7,8] or biological [6] systems stems from the presence of short-range attractions and long-range repulsions in their effective interaction potential. Whereas the former provide the driving force for unlimited cluster growth, the latter act as a barrier against it that brings further particle aggregation to an end [3,7]. Cluster formation is a highly topical issue due to the large variety of cluster morphologies that form [5,9,11] and to the relevance of these structures in influencing vitrification and gelation [5,9,12].

In this Letter, we report on a different mechanism that gives rise to a distinct type of cluster formation, and which does not rest on the explicit existence of competing interactions. Contrary to the cases in Refs. [5–8], the constituent particles we consider are allowed to overlap and are purely repulsive. Both conditions are readily fulfilled for various types of polymeric macromolecules, e.g., polymer chains [13], polyelectrolytes [14], or dendrimers [15]. Under certain, general conditions on the properties of the Fourier transform $\tilde{\Phi}(q)$ of the interparticle potential $\Phi(r)$, we demonstrate that the particles form aggregates that further organize into regular cluster crystals with multiple site occupancy. We explicitly confirm the theoretical results by performing extensive computer simulations on a specific system that represents the entire class of effective interactions [16].

Ultrasoft effective interactions [2,17] hide many surprises in the topology of their phase diagrams and the types of crystal phases that arise, even for purely isotropic pair potentials $\Phi(r)$ [18–20]. For the case in which $\Phi(r)$ is non-negative and bounded, a general criterion determining the *topology* (but not the crystal structures) of the phase diagram has been put forward [16]. If the Fourier transform $\tilde{\Phi}(q)$ is non-negative (termed Q^+ class), then the system displays reentrant melting with an upper freezing temperature. If, on the other hand, $\tilde{\Phi}(q)$ oscillates around zero (termed $Q^\pm$ class), then a transition into an ordered cluster phase will take place at arbitrary temperatures. This corresponds exactly to the ordered "clump phase" described in Ref. [21]. The argument put forward in Ref. [16] rests on the fact that, except at small densities and temperatures, the fluid state of the systems at hand is extremely well described by the mean-field approximation (MFA) $c(r) = -\beta\Phi(r)$, where $c(r)$ is the direct correlation function and $\beta = (k_B T)^{-1}$, with Boltzmann's constant k_B and the absolute temperature T. Consequently, the fluid structure factor $S(q)$ is given by $S(q) = [1 + \beta\rho\tilde{\Phi}(q)]^{-1}$, where ρ denotes the number density. Consider now the $Q^\pm$ class and let q_* be the wave vector for which $\tilde{\Phi}(q)$ attains its minimum, *negative* value. Then, $S(q)$ develops a real pole at q_* along the so-called λ line [16,22,23], which signals an instability of the uniform phase. Evidently, the λ line has the shape $k_B T_\lambda = |\tilde{\Phi}(q_*)|\rho_\lambda$; i.e., it persists at all temperatures. Since q_* is set solely by the interaction, the crystal lattice constant $a \propto q_*^{-1}$ should be density independent, at least on the freezing line. Thus, the number of particles in the elementary cell should change accordingly, a requirement that can be fulfilled by the formation of multiparticle aggregates (clusters).

Although the reentrant melting scenario has been confirmed [20,24–26], the clustering scenario has received considerably less attention up to now. In this work, we explicitly demonstrate its validity. We perform a detailed investigation of the generalized exponential model of index n (GEM-n), $\Phi(r) = \varepsilon \exp[-(r/\sigma)^n]$, with $n = 4$. It can be shown that $\Phi(r)$ belongs to the Q^+ class for $n \le 2$ and to the $Q^\pm$ class for $n > 2$. For $n = 2$, the Gaussian core model of Stillinger [27] is recovered. The GEM-4 is treated here as a representative of the $Q^\pm$ class. Suitably tailored dendrimers that have been assembled in a computer simulation show evidence for a GEM-n-type of effective interaction with $n > 2$; hence this model reflects the behavior of realistic systems [28].

We define $\rho^* \equiv \rho\sigma^3$ and $T^* \equiv k_B T/\varepsilon$. Our investigations consist of a combination of sophisticated minimization algorithms, density functional theory (DFT), and advanced Monte Carlo (MC) simulations. We start with a calculation at $T = 0$, allowing for the formation of clusters in which n_c particles sit on top of each other, and minimize the lattice sum with respect to the crystal structure and n_c. Since the periodic lattice that the clusters form is *a priori* unknown, we take advantage of an unbiased search strategy based on genetic algorithms [29]. Only fcc and bcc crystals were predicted, which are used as candidates at finite temperatures. For this purpose, we employ DFT with the highly accurate MFA-excess free energy [23,25,30,31] $\mathcal{F}_{\rm ex}[\rho] = (1/2)\int d\mathbf{r}_1 \int d\mathbf{r}_2 \rho(\mathbf{r}_1)\rho(\mathbf{r}_2)\Phi(|\mathbf{r}_1 - \mathbf{r}_2|)$. For the one particle density, $\rho(\mathbf{r})$, we made the Gaussian ansatz $\rho(\mathbf{r}) \equiv \sum_{\{\mathbf{R}_i\}}\rho_{\rm cl}(\mathbf{r} - \mathbf{R}_i) = n_c(\alpha/\pi)^{3/2}\sum_{\{\mathbf{R}_i\}} e^{-\alpha(\mathbf{r}-\mathbf{R}_i)^2}$, where $\rho_{\rm cl}(\mathbf{r})$ is the cluster density profile and the vectors $\{\mathbf{R}_i\}$ form a Bravais lattice [32]. The total free energy is $\mathcal{F}[\rho] = \mathcal{F}_{\rm id}[\rho] + \mathcal{F}_{\rm ex}[\rho]$, with the ideal part $\mathcal{F}_{\rm id}[\rho] = k_B T \int d\mathbf{r}\rho(\mathbf{r})[\ln(\rho(\mathbf{r})\Lambda^3) - 1]$, Λ being the thermal de Broglie wavelength. For $\alpha\sigma^2 \gtrsim 20$, $F_{\rm id}$ can be approximated analytically and the variational free energy, $F/N \equiv f(n_c, \alpha)$, takes the form:

$$f(n_c, \alpha) = k_B T[\ln n_c + 3\ln(\sqrt{\alpha\sigma^2/\pi})] + n_c\sqrt{\frac{\alpha}{8\pi}}\sum{}' \int_0^\infty dr \frac{r}{R_i}[e^{-\alpha(r-R_i)^2/2} - e^{-\alpha(r+R_i)^2/2}]\Phi(r)$$
$$+ (n_c - 1)\sqrt{\frac{\alpha^3}{8\pi}}\int_0^\infty dr r^2 e^{-\alpha r^2/2}\Phi(r) + 3k_B T\ln(\Lambda/\sigma), \qquad (1)$$

where the primed sum is carried over all lattice vectors excluding $\mathbf{R} = \mathbf{0}$, $R_i = |\mathbf{R}_i|$. The function $f(n_c, \alpha)$ is then minimized at any state point with respect to n_c and α. For a given crystal (fcc or bcc) and density ρ^*, the cluster population n_c and the lattice vector lengths R_i are coupled to one another, $R_i/\sigma \propto l_i(n_c/\rho^*)^{1/3}$, where l_i are lattice-specific numerical coefficients. At the *minimum* of $f(n_c, \alpha)$, which corresponds to a *mechanically* stable crystal, the particular property $n_c \propto \rho^*$ is fulfilled, so that the lattice constants of both the bcc and the fcc lattices remain fixed at all ρ^* values. In particular, the nearest neighbor distances for bcc and fcc have the values $d_{\rm bcc} = 1.368\sigma$ and $d_{\rm fcc} = 1.414\sigma$, respectively.

In order to check the *thermodynamic* stability of the crystals as well, we calculated the free energy of the uniform fluid employing the MFA, $c(r) = -\beta\Phi(r)$, as a closure to the Ornstein-Zernike relation and following the energy route to thermodynamics. The resulting phase diagram is shown in Fig. 1. At low densities, the system is fluid. Upon compression, a first-order clustering transition occurs, leading at sufficiently high densities to the fcc structure. Above the triple temperature, $T_t^* \cong 0.4$, a wedge-shaped cluster bcc region intervenes between the fluid and the cluster fcc. Thus, the system also shows polymorphic transitions between cluster solids. The bcc-fcc density gap is very narrow, contrary to the fluid-crystal gap. In agreement with Ref. [16], the freezing and melting curves are almost straight lines that preempt the λ line.

To put the theoretical predictions in a stringent test, we also carried out MC simulations in the *NVT* ensemble. Typically we used systems with approximately 5000 particles and extended the computer experiments to 150 000 MC sweeps. Considerable speedup was achieved by implementing a discretized simulation technique [33]. The symmetry of the resulting regular structures was analyzed

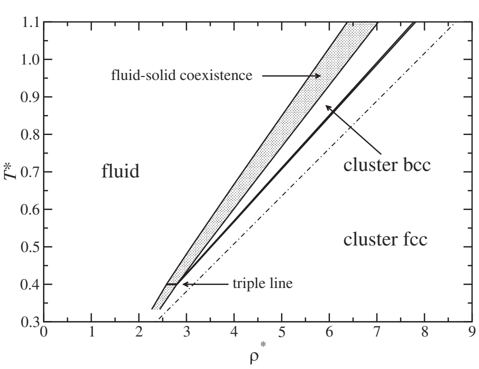

FIG. 1. The phase diagram of the GEM-4 model, as obtained by DFT. The shaded area represents the coexistence region of the liquid and the cluster bcc phase. The dash-dotted curve is the λ line of the system, calculated in the MFA.

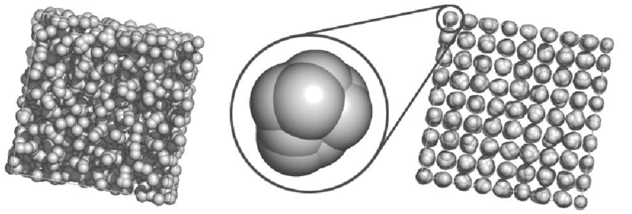

FIG. 2. Two simulation snapshots of a GEM-4 system for $T^* = 0.4$ and $\rho^* = 2.5$ and 7 (left and right). The middle panel shows a close-up of one cluster. Particle diameters are not drawn to scale but are chosen to optimize the visibility of the structures.

as proposed in Ref. [34]. In the simulations, we found evidence of spontaneous clustering and crystallization, which is demonstrated by the snapshots in Fig. 2, both for $T^* = 0.4$. Whereas in the left panel ($\rho^* = 2.5$) the system is obviously in the fluid phase, formed by isolated particles as well as clusters, at a higher density $\rho^* = 7.0$, in the right panel, the particles are tightly bound in clusters that are located on a fcc lattice.

To determine the chemical potential μ we used Widom's particle insertion [35] supplemented by the overlapping distribution method [35], and the free energies $F_{\rm bcc}$ and $F_{\rm fcc}$ were obtained via the Gibbs-Duhem relation. A compilation of DFT and MC results for the free energies of all phases at $T^* = 1$ is shown in Fig. 3. It can be seen that the DFT results are in excellent agreement with simulations, a fact that amply confirms the accuracy of the former and of the phase diagram in Fig. 1. In the inset of Fig. 3 we show a close-up of the three-phase region, to demonstrate that the cluster bcc crystal is not preempted by a transition between fluid and cluster fcc. Spontaneous polymorphic bcc → fcc transitions were not observed within the simulation but they can be forced in isotension ensemble simulations.

In addition, we have measured in the simulations in the solid phases the mean occupancy of the clusters, $\langle N_c \rangle$, where N_c is the number of particles in one specific cluster, and compared it with n_c obtained from DFT. Representative results for $T^* = 1$ are shown in Fig. 4, showing excellent agreement between the two. The linear dependence of n_c on ρ^* is fully confirmed (Fig. 4, left inset). There is only a tiny difference in the population of the bcc and fcc clusters, leading to a ratio $d_{\rm fcc}/d_{\rm bcc} = 1.034$, very close to the value $\sqrt[6]{2^5}/\sqrt{3} \cong 1.029$ obtained when n_c is identical for both lattices. At fixed ρ^*, n_c is also practically T^* independent. In the right inset of Fig. 4, we show the probability distribution of N_c as obtained by MC simulations for $\rho^* = 6.5$ (left curve) and 9 (right curve): the variation ΔN_c shrinks as the density increases.

The clusters become more compact with increasing density, as witnessed by the increase of the α values. As can be seen in Fig. 5, the DFT-Gaussian density profile is in excellent agreement with the one measured in MC. It appears that α also has a linear dependence on ρ^*. This property is intricately related to cluster formation and can be understood as follows. Let us fix all particles but one on their lattice sites and consider the site potential $V(\mathbf{r})$ they exert on this test particle, which oscillates around $\mathbf{r} = \mathbf{0}$. Taking only the m nearest neighbor sites into account, we have $V(\mathbf{r}) = (n_c - 1)\Phi(r) + n_c \sum \Phi(|\mathbf{r} - \mathbf{R}_{\rm nn}|)$, where the sum runs over all nearest neighbor clusters, located at the vectors $\mathbf{R}_{\rm nn}$ of length d. For small r, we can write $V(\mathbf{r}) \cong V(0) + (1/2)mn_c\Phi''(d)r^2$, since $\Phi''(0) = 0$ [36]. Thus, the density profile $\rho(\mathbf{r}) \propto \exp[-\beta mn_c\Phi''(d)r^2/2]$ results, hence $\alpha = \beta mn_c\Phi''(d)/2$. Since $n_c \propto \rho^*$, $\alpha \propto \rho^*$ also follows. From these considerations, we also conclude that particles are able to hop between clusters. At $\rho^* = 7.5$ and $T^* = 1$, the energy barrier between sites is just $\approx 3.2k_{\rm B}T$. The barrier height grows with ρ^*, rendering particle hopping less and less probable. Particle motions within a cluster should be largely uncorrelated, as the flat shape of $\Phi(r)$ at $r = 0$ yields very weak intracluster forces.

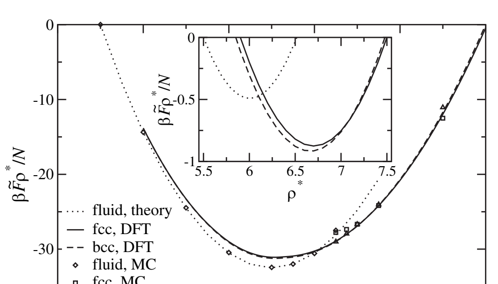

FIG. 3. DFT and MC results for the modified free energy density $\beta\tilde{F}\rho^*/N \equiv \beta F\rho^*/N + K_1\rho^*$ of the GEM-4 system against ρ^* at $T^* = 1$. A thermodynamically irrelevant term $K_1\rho^*$ has been added for clarity of presentation. The error bars of the MC results are smaller than the symbol size. Inset: a close-up on the region of stability of the cluster bcc lattice. Here, a different linear term $K_2\rho^*$ has been added.

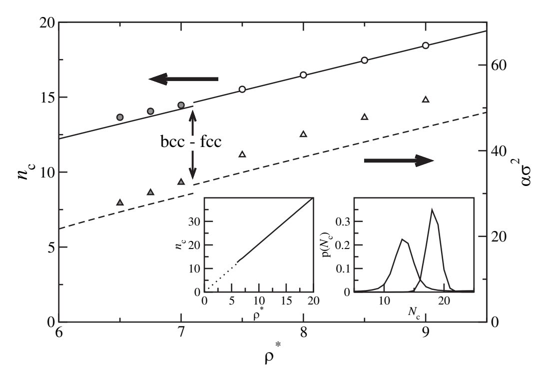

FIG. 4. Cluster size n_c and localization parameter $\alpha\sigma^2$, for the GEM-4 system at $T^* = 1$, plotted against the density ρ^*. Lines: DFT results, points: MC simulations. There are small discontinuities at the density of the bcc-fcc transition. The left inset shows DFT results that corroborate the $n_c \propto \rho^*$ relation. The dashed part of the line is an extrapolation to low densities, for which the crystal is unstable. The right inset shows the probability distribution of cluster population N_c from simulations at $\rho^* = 6.5$ (left curve) and $\rho^* = 9$ (right curve).

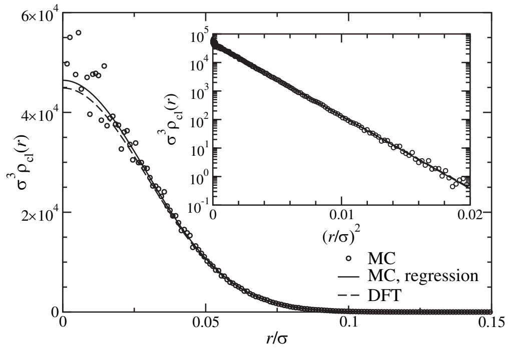

FIG. 5. Cluster density profile $\rho_{\mathrm{cl}}(r)$ of the GEM-4 system at $T^* = 0.1$ and $\rho^* = 9$. Inset: Semilogarithmic plot of $\rho_{\mathrm{cl}}(r)$ against r^2, demonstrating the Gaussian shape of the former.

All salient properties of the GEM-4 model that drive cluster formation are common to the entire $Q^{\pm}$ class, thus the phenomena presented here should be general. The spontaneous formation of clusters appears counterintuitive at first sight as, indeed, it occurs at the complete absence of competing interactions at the level of the pair potential. The underlying reason is rather the emergence of competing trends in the free energy, as can be seen in Eq. (1). The entropy loss due to particle aggregation and the "self-interaction" within the cluster [the $k_{\mathrm{B}}T \ln n_c$ term and the second to last term on the right hand side of Eq. (1), respectively] disfavor the growth of n_c. However, increasing n_c also entails the gain in avoiding close contacts with the nearest neighbors, due to the concomitant increase of the lengths R_i in the second term on the right hand side of Eq. (1). At the same time, excessive growth of n_c is also unfavorable, because it drives the interneighbor interaction term to zero, as the R_i's then lie outside the range of $\Phi(r)$: the entropic and self-interaction terms overtake as $n_c \to \infty$ and stop further aggregation. Interactions with the neighbors are also indispensable for the mechanical stability of the crystals, providing the required restoring forces for particle oscillations around the lattice sites. The stability of the clusters against both decomposition to $n_c = 1$ and unlimited growth towards $n_c \to \infty$ is therefore seen to arise from a competition between *intra*-cluster interaction and entropy, on the one hand, and *inter*-cluster interaction, on the other. The necessary requirements for this scenario are that $\Phi(r)$ is bounded (to allow full overlaps) and that it falls rapidly enough to zero for $r \to \infty$, so that $\tilde{\Phi}(q)$ develops oscillations that give rise to the λ line.

We have presented a detailed analysis of the phase behavior of a particular soft-interaction system representative of a broad class of effective interaction potentials that are realistic for ultrasoft, polymeric colloids. A novel mechanism for the development of cluster phases has been demonstrated to be at work, which gives rise to polymorphic crystals with unusual structural properties. The system is accurately described by a mean-field density functional, as confirmed by comparison with computer simulations. Work along the lines of tailoring dendrimers that show $Q^{\pm}$ interactions is under way. Future directions include the investigation of anomalous diffusion, gelation, and vitrification of such systems.

We thank H. Fragner, D. Frenkel, and J. C. Pàmies for helpful discussions. This work was supported by the Österreichische Forschungsfond, Project No. P15758 and No. P17823, by the DFG within the SFB-TR6 and by the HPC-EUROPA Project (RII3-CT-2003-506079).

[1] W. B. Russel, D. A. Saville, and W. R. Schowalter, *Colloidal Dispersions* (Cambridge University Press, Cambridge, England, 1990).
[2] C. N. Likos, Phys. Rep. **348**, 267 (2001).
[3] D. Frenkel, see link http://www.bell-labs.com/jc-cond-mat/june/jccm_jun04_03.html
[4] P. N. Segrè *et al.*, Phys. Rev. Lett. **86**, 6042 (2001).
[5] F. Sciortino *et al.*, Phys. Rev. Lett. **93**, 055701 (2004).
[6] A. Stradner *et al.*, Nature (London) **432**, 492 (2004).
[7] S. Mossa *et al.*, Langmuir **20**, 10 756 (2004).
[8] A. I. Campbell *et al.*, Phys. Rev. Lett. **94**, 208301 (2005).
[9] R. Sanchez and P. Bartlett, J. Phys. Condens. Matter **17**, S3551 (2005).
[10] E. Stiakakis *et al.*, Europhys. Lett. **72**, 664 (2005).
[11] F. Sciortino *et al.*, J. Phys. Chem. B **109**, 21 942 (2005).
[12] F. Sciortino and P. Tartaglia (to be published).
[13] A. A. Louis *et al.*, Phys. Rev. Lett. **85**, 2522 (2000).
[14] M. Konieczny *et al.*, J. Chem. Phys. **121**, 4913 (2004).
[15] I. O. Götze *et al.*, J. Chem. Phys. **120**, 7761 (2004).
[16] C. N. Likos *et al.*, Phys. Rev. E **63**, 031206 (2001).
[17] S. H. L. Klapp *et al.*, J. Phys. Condens. Matter **16**, 7331 (2004).
[18] M. Watzlawek, C. N. Likos, and H. Löwen, Phys. Rev. Lett. **82**, 5289 (1999).
[19] P. Ziherl and R. Kamien, Phys. Rev. Lett. **85**, 3528 (2000).
[20] D. Gottwald *et al.*, Phys. Rev. Lett. **92**, 068301 (2004).
[21] W. Klein *et al.*, Physica (Amsterdam) **205A**, 738 (1994).
[22] R. Finken *et al.*, J. Phys. A **37**, 577 (2004).
[23] A. J. Archer *et al.*, J. Phys. Condens. Matter **16**, L297 (2004).
[24] F. H. Stillinger and D. K. Stillinger, Physica (Amsterdam) **244A**, 358 (1997).
[25] A. Lang *et al.*, J. Phys. Condens. Matter **12**, 5087 (2000).
[26] S. Prestipino, F. Saija, and P. V. Giaquinta, Phys. Rev. E **71**, 050102 (2005).
[27] F. H. Stillinger, J. Chem. Phys. **65**, 3968 (1976).
[28] B. M. Mladek *et al.* (unpublished).
[29] D. Gottwald *et al.*, J. Chem. Phys. **122**, 204503 (2005).
[30] A. A. Louis, P. G. Bolhuis, and J. P. Hansen, Phys. Rev. E **62**, 7961 (2000).
[31] L. Acedo and A. Santos, Phys. Lett. A **323**, 427 (2004).
[32] A. J. Archer, Phys. Rev. E **72**, 051501 (2005).
[33] A. Z. Panagiotopoulos, J. Chem. Phys. **112**, 7132 (2000).
[34] P. J. Steinhardt, D. R. Nelson, and M. Ronchetti, Phys. Rev. B **28**, 784 (1983).
[35] D. Frenkel and B. Smit, *Understanding Molecular Simulation* (Academic Press, London, 2002), 2nd ed.
[36] Valid for the $Q^{\pm}$ members of the GEM-n family, $n > 2$. For $n \leq 2$, the term $(n_c - 1)\Phi''(0)$ renders $V''(0) < 0$ for $n_c > 1$, hence clustering does not lead to stable crystals.